Mid-Infrared Intersubband Absorption from p-Ge Quantum Wells Grown on Si Substrates

K. Gallacher[a], A. Ballabio[b], R. Millar[a], J. B. J. Frigerio[b], A. Bashir[c], I. MacLaren[c], G. Isella[b], M. Ortolani[d], and D. J. Paul[a]

[a]University of Glasgow, School of Engineering, Rankine Building, Oakfield Avenue, Glasgow, G12 8LT, U.K
[b]University of Glasgow, School of Physics and Astronomy, Kelvin Building, University Avenue, Glasgow G12 8QQ, U.K.
[c]L-NESS, Dipartimento di Fisica del Politecnico di Milano, Polo Territoriale di Como, Via Anzani 42, I-22100 Como, Italy
[d]Center for Life NanoScience@Sapienza, Istituto Italiano di Tecnologia, Viale Regina Elena 291, I-00161 Rome, Italy

Mid-infrared intersubband absorption from p-Ge quantum wells with $Si_{0.5}Ge_{0.5}$ barriers grown on a relaxed $Si_{0.2}Ge_{0.8}$ buffer on a Si substrate is demonstrated from 6 to 9 μm wavelength at room temperature and can be tuned by adjusting the quantum well thickness. Fourier transform infra-red transmission demonstrate clear absorption peaks corresponding to intersubband transitions among confined hole states. The work indicates an approach that will allow quantum well intersubband photodetectors to be realized on Si substrates in the important atmospheric transmission window of 8-13 μm where many chemical and biological molecules have unique molecular absorption lines for spectroscopic identification.

Introduction

There are many applications in the mid-infrared part of the electromagnetic spectrum such as thermal imaging and the unique identification of molecules through absorption spectroscopy [1-4]. For all these applications, sources of mid-infrared light and photodetectors are key to enable any application. III-V and II-VI semiconductor materials have dominated over the last decades with both interband and intersubband emission and/or absorption devices [5] but there is now significant interest in developing technology on silicon substrates to enable far cheaper systems for mass-market applications in environmental sensing, personalized healthcare, and security [6-7]. SiGe quantum well (QW) intersubband photodetectors (QWIPs) have also been previously demonstrated but the number of QWs was limited by the SiGe critical thickness thereby limiting performance [8-9]. Recently, it has been demonstrated that p-Ge QWs can provide strong absorption in the 8-13 μm wavelength range through intersubband absorption [10]. These p-Ge QW superlattice structures can be strain symmetrised [4] past the critical thickness limitations of a single heterolayer and therefore provide large absorption coefficients. In this paper, we present the design, growth, and experimental characterization of 5.4, 8.1, and 9.2 nm thick p-Ge QW superlattice structures.

Experiment

The band energies and confined wave-functions were calculated using a self-consistent 8-band **k.p** Poisson-Schrödinger solver with periodic boundary conditions orientated along the growth-axis and the deformation potentials from ref [11]. Figure 1 presents the calculated band structure for a 5.4 nm Ge QW and 3.6 nm $Si_{0.5}Ge_{0.5}$ barriers on a relaxed $Si_{0.2}Ge_{0.8}$ buffer. The ground state in the QW is HH1 due to strain splitting of the HH and LH bands. The HH2 and HH3 are at roughly the same energy as the LH1 and LH2 subband states, respectively. For a doping level of $N_A \approx 10^{18}$ cm^{-3} within the QW, the Fermi level at room temperature sits at the HH2 band. Therefore, the HH2-HH3 intersubband transition should be optically active. The designed Ge QW structures were grown by low-energy plasma-enhanced chemical vapor deposition on high resistivity Si (100) to reduce free-carrier absorption from the substrate [10, 12-13]. A 500 nm thick $Si_{0.6}Ge_{0.4}$ layer was first grown followed by a 500 nm linear graded buffer from x = 0.4 until x = 0.8. Then an undoped 10 nm $Si_{0.2}Ge_{0.8}$ spacer region was grown followed by the evenly doped active region ($N_A \approx 10^{18}$ cm^{-3}) consisting of 500 periods of compressively strained Ge QWs (tensile strained $Si_{0.5}Ge_{0.5}$ barriers) of 5.4 (3.6), 8.1 (5.4), and 9.2 (6.1) nm thickness. Lastly, another undoped 10 nm $Si_{0.2}Ge_{0.8}$ spacer layer was grown, followed by a 20 nm $Si_{0.2}Ge_{0.8}$ cap region.

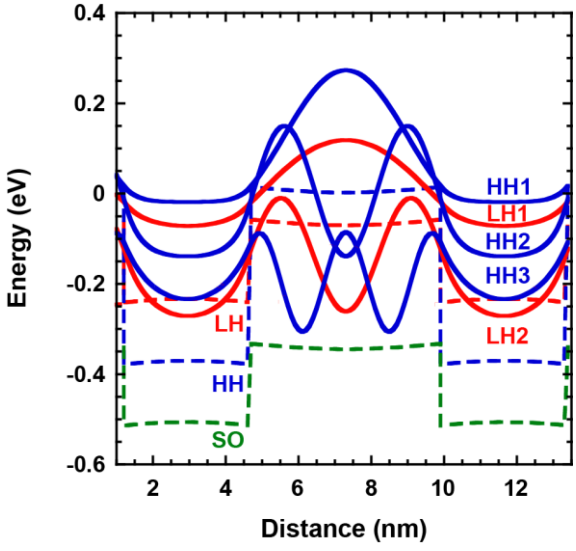

Figure 1. A schematic diagram of the calculated band structure for a 5.4 nm wide Ge quantum well sandwiched between 3.6 nm $Si_{0.5}Ge_{0.5}$ barriers. The squared wave-functions (solid lines) for the lowest energy subband states for the heavy hole (HH) and light hole (LH) bands are presented along with the hole band edges (dashed lines).

Heterolayer thicknesses of the grown superlattice structures were measured by scanning transmission electron microscopy (STEM). The STEM was performed on a probe-corrected JEOL ARM 200F equipped with a cold field emission gun operated at 200 kV. A Gatan GIF Quantum ER energy filter/ spectrometer equipped with a fast dual electron energy loss spectroscopy (EELS) system was used. The STEM was operated in high angle annular dark field mode (HAADF). Atomic (Z) contrast image was obtained by the detection of elastically and quasi-elastically scattered electrons using a HAADF. Therefore, this is a well-suited method for imaging Ge and SiGe interfaces. The HADDF STEM image in Figure 2(a) demonstrates the smooth and abrupt interfaces between the

Ge QWs and the $Si_{0.5}Ge_{0.5}$ barriers for the 8.1 nm QW superlattice structure. Figure 2 (b) reveals that there is a slight variation of the QW and barrier thicknesses throughout the superlattice growth and therefore the thicknesses stated are the calculated average.

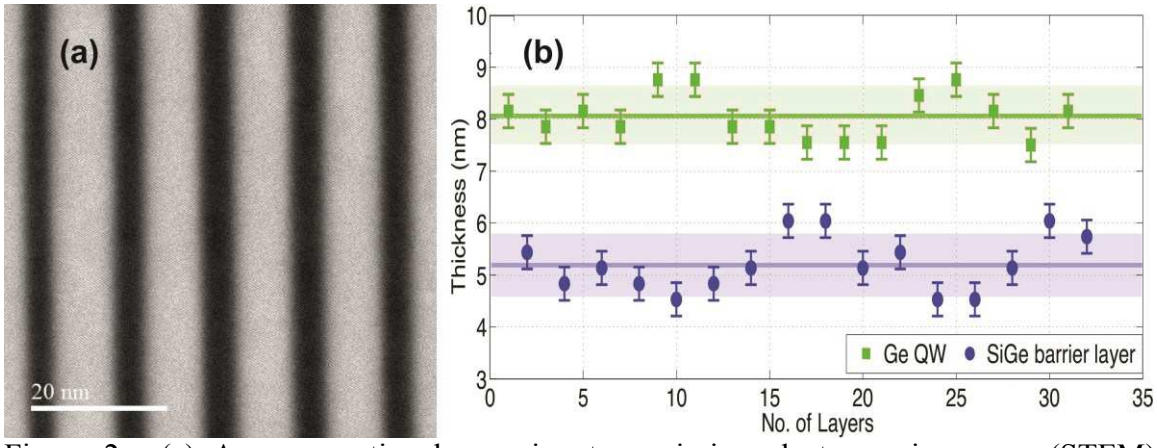

Figure 2. (a) A cross-sectional scanning transmission electron microscope (STEM) image of the 8.1 nm Ge quantum well structure by high angle annular dark field mode STEM image at 3 million times magnification. Due to the Z^2 dependence, heavier atoms appear brighter because of strong scattering at high angles while lighter atoms appear darker. Therefore lighter regions in this image correspond to Ge QWs and the darker regions correspond to the SiGe barriers. (b) Thickness variation of the superlattice structure as obtained from STEM analysis. In this case the Ge QWs have an average thickness of ~ 8.1 nm (green line) and the SiGe barriers are ~ 5.2 nm thick (blue line).

Fourier transform infrared (FTIR) transmission measurements were performed on the as-grown QW structures in vacuum at temperatures ranging from 6 to 300 K. The setup consisted of a Bruker IFS 66v interferometer and a nitrogen-cooled MCT detector operated in step-scan mode [14]. The normalized FTIR absorption spectra at 300 K in vacuum for the 5.4, 8.1, and 9.2 nm QW structures is demonstrated in Figure 3(a). The absorption peak at ~9 μm wavelength corresponds to vibrational interstitial oxygen impurities in the Si substrate. The QW design was for a bound-to-continuum transition from the HH2 to the mixed LH continuum formed from weakly / unconfined LH2 state that mixes with the HH3 bound state.

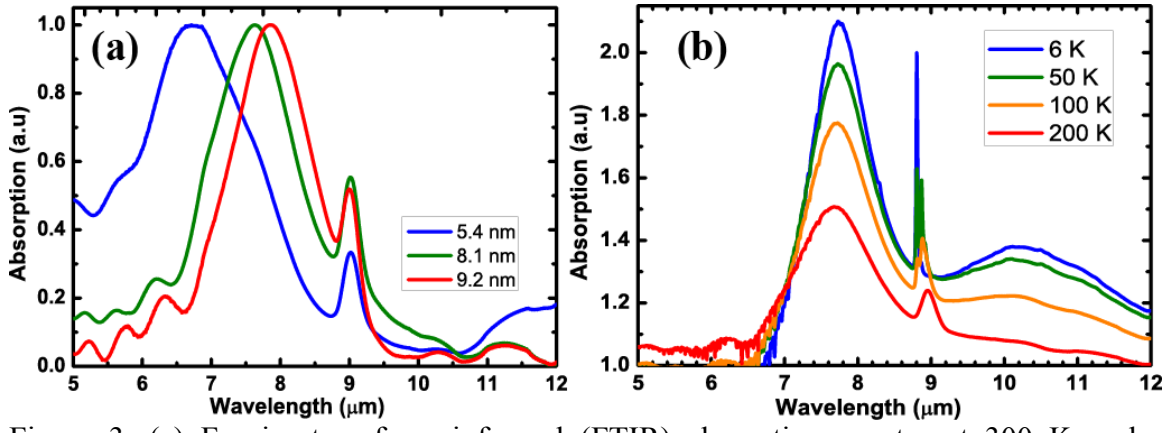

Figure 3. (a) Fourier transform infra-red (FTIR) absorption spectra at 300 K under vacuum for the as-grown 5.4, 8.1, and 9.2 nm Ge quantum well (QW) structures. (b) The low temperature FTIR absorption spectra of the 8.1 nm QW structure from 6-200 K.

The low temperature (6-200 K) absorption spectra of the 8.1 nm QW structure is demonstrated in Figure 3(b). It is clear from Figure 3(b) that as the temperature decreases the intersubband absorption is increasing. There is a negligible intersubband absorption temperature dependence observed. This results from the fact that both the band-edges of the barriers and QWs are changing at approximately the same rate in energy as the temperature changes and produce a negligible change in terms of the QW depth for both the HH and LH bands. It is also evident from the spectra that there is a longer wavelength absorption peak appearing with decreasing temperature at ~ 10.2 μm wavelength. Most likely, the Fermi level enters the HH1 subband at low temperature, activating the HH1-HH2 transition. Doping-dependent analysis will be required to address this point further.

Conclusions

In conclusion, intersubband absorption from p-Ge QWs of different widths designed by an 8-band **k.p** self-consistent Poisson-Schrödinger tool has been demonstrated. High quality growth of the Ge QWs has been confirmed by STEM analysis. FTIR transmission spectroscopy displayed absorption peaks corresponding to intersubband transitions between subband states within the QW. The absorption shifts to lower wavelengths for thinner QWs as expected. This work demonstrates surface-normal intersubband absorption from p-Ge QWs that occurs in the important atmospheric transmission window of 8-13 μm. It is envisaged that such designs could produce surface normal and waveguide coupled photodetectors for spectroscopic sensing in the MIR.

Acknowledgments

The research leading to these results has received funding from the European Union's Seventh Framework Programme under grant agreement no. 613055 and U.K. EPSRC (Project no. EP/N003225/1). The authors would like to thank the staff of the James Watt Nanofabrication Centre for help in fabricating the devices used in this work.

References

1. L. Baldassarre, et al., *Nano Lett.* **15**, 7225 (2015).
2. P. Biagioni, et al., *J. Nanophoton.* **9**, 093789 (2015).
3. D.J. Paul, *Elec. Lett.* **45**, 582 (2009).
4. D.J. Paul, *Laser Photon. Rev.* **4**, 610 (2010).
5. A. Rogalski, *J. Appl. Phys.* **93**, 4355 (2003).
6. R.W. Millar, et al., *Opt. Express* **23**, 18193 (2015).
7. R.W. Millar, et al., *Opt. Express* **24**, 4365 (2016).
8. R.P.G. Karunasiri, et al., *Appl. Phys. Lett.* **57**, 2585 (1990).
9. J.S. Park, R.P.G. Karunasiri, and K.L. Wang, *Appl. Phys. Lett.* **61**, 681 (1992).
10. K. Gallacher, et al., *Appl. Phys. Lett.* **108**, 091114 (2016).
11. D. J. Paul, *Phys. Rev. B* **77**, 155323 (2008).
12. G. Isella, et al., *Solid-State Electron.* **48**, 1317 (2004).
13. F. Pezzoli, et al., *Appl. Phys. Lett.* **108** 262103 (2016).
14. S.A. Lynch, et al., *Appl. Phys. Lett.* **81**, 1543 (2002).